DOI https: //doi. org/10.1007/s11595-018-1814-z

Preparation of Magnetic Fluorescent Dual-drug Nanocomposites for Codelivery of Kaempferol and Paclitaxel

ZHANG Xiaojuan[1], PAN Qingqing[2], HAO Lingyun[1*], LIN Qing[1], TIAN Xiangping[1], ZHANG Zhiying[1], WANG Shanshan[3], WANG Hehe[1]

(1. School of Material Engineering, Jinling Institute of Technology, Nanjing 211169, China; 2. College of Chemical Engineering, Nanjing Forestry University, Nanjing 210037, China; 3. Laboratory Animal Center, Nanjing University of Chinese Medicine, Nanjing 210023, China)

Abstract: Magnetic fluorescent dual-drug nanocomposites (MFDDs) were developed with the aim of simultaneouly delivering two different anticancer drugs, kaempferol (KAE) and paclitaxel (PTX). Firstly, Fe_3O_4/bovine serum albumin (Fe_3O_4/BSA) composite microspheres with physically entrapped KAE were prepared, then microspheres were modified with PTX/graphene quantum dots (PTX/GQDs) through chemically bonding, and the MFDDs were obtained. The properties of nancomposites were characterized by X-ray diffractometry, Fourier-transform infrared spectroscopy, transmission electron microscopy, vibrating sample magnetometry and X-ray fluorescence spectrometry. It was found that the superparamagnetic nanocomposites had ultrafine size (below 110 nm), high saturation magnetization of 24.36 emu/g, and significant fluorescence. Furthermore, the cumulative *in vitro* release of the MFDDs exhibited controlled drug release. Cell viability experiments confirmed that the co-administration of KAE with PTX had a superior cytotoxicity to the Hela cells compared with single drug-loaded forms. Therefore, dual anticancer drug-loaded MFDDs have the potential to be used for cancer combined chemotherapy.

Key words: dual-drug delivery; nanocomposites; graphene quantum dots; kaempferol; paclitaxel; Hela cells

1 Introduction

Carcinoma affects millions of individuals and is responsible for many million deaths annually worldwide[1]. Single agent therapy has seen limited success in cancer treatment due to the toxicity at high drug dosage, the heterogeneity of cancer cells and the drug resistance[2]. Conventional drug carriers are utilized to entrap single therapeutic agent, but in practical applications, combination delivery of multi-drugs or any other therapeutic agents is required to deal with complicated cases. Therefore, the design and synthesis of dual-drug delivery systems (DDDs) will be effective in the treatment of cancer[3].

To date, various DDDs have been developed to improve therapy efficacy. Salehi *et al* developed smart thermo/pH responsive magnetic nanogels for co-delivery doxorubicin (DOX) and methotrexate (MTX), which had a superior cytotoxicity to MCF7 cells compared with single drug-loaded forms[4]. Huang *et al* established a novel mixed micelle to simultaneously delivery chemical bonded DOX and physical entrapped PTX, which showed strong anti-tumor activity[5]. Pradhan *et al* constructed thin lipid layer coated mesoporous magnetic nanoassemblies for delivering DOX and PTX, which had a greater cytotoxicity effect in Hela and MCF-7 cancer cells[6]. Ashwanikumar *et al* synthesized copolymeric nanomicelles for co-delivery of 5-fluorouracil (5-FU) and methotrexate (MTX), which had promising action to treat colon cancer[7]. It has also been found that the combination of two drugs shows synergistic effects, prevents more disease recurrence and increases tumor regression capabilities compared to individual drugs in clinical studies[8].

Kaempferol (KAE) is a natural compound, extracted from the berries, brassica and allium species. In recent years it has attracted considerable attention due to its anti-cancer properties, which exhibits good inhib-

(Received: Dec. 21, 2016; Accepted: Oct. 25, 2017)

ZHANG Xiaojuan (张小娟): Assoc. Prof.; Ph D; E-mail: xixi@jit.edu.cn

*Corresponding author: HAO Lingyun(郝凌云): Prof.; Ph D; E-mail: xixi1005@hotmail.com.

Funded by the Natural Science Fund of Jiangsu Overseas Research & Training Program for University Prominent Young & Middle-aged Teachers and Presidents, the Natural Science Fund of Jiangsu Province (No.BK20130094), the Enterprise-universities Cooperative Innovation Fund of Jiangsu Province (No. BY2014016) and the National Natural Science Foundation of China (No.51103066)

itory effect on cervix carcinoma cells[9-10]. Paclitaxel (PTX) is one of the first-line chemotherapeutics used to treat patients with cancer, and the application of PTX in the clinic has been limited by its poor water solubility and the systemic toxicity[11]. It has been reported that kaempferol can markedly increase the sensitivity of the multidrug-resistant human cervical carcinoma cells to paclitaxel, and also decrease the drug resistance of paclitaxel in cervical carcinoma cells[12]. Thus, there is a need to develop DDDs for co-delivery of KAE and PTX.

Graphene quantum dots (GQDs) are more environmentally friendly, biocompatible and photostable compared with conventional semiconductor quantum dots, which could be used for drug delivery and imaging[13-15]. Functionalized magnetic microspheres are universally employed for conjugation with biomolecules and drugs[16-18]. In this paper, we reported magnetic fluorescent dual-drug nanocomposites (MFDDs) for co-delivery of KAE and PTX with GQDs as fluorescent materials. The structure, morphology, magnetic property, fluorescence, and drug releasing property of MFDDs were also determined. In addition, the inhibitory effect of MFDDs on Hela cells was evaluated by *in vitro* cytotoxicity.

2 Experimental

2.1 Materials

The cyclohexane-based Fe_3O_4 ferrofluids were self-prepared using the modified chemical coprecipitation[19], and amino-functionalized green graphene quantum dots (GQDs-NH_2) were self-prepared using the hydrothermal method[20]. Kaempferol (KAE) and paclitaxel (PTX) were obtained from Sigma Aldrich. The other reagents were obtained from commercial source and used without further purification.

2.2 Preparation of magnetic fluorescent dual-drug nanocomposites

2.2.1 Preparation of magnetic microspheres loading with KAE

Firstly, 1 g BSA was dissolved in 50 mL distilled water. Then 5 mg KAE was dissolved in 2 g cyclohexane-based Fe_3O_4 ferrofluids, and the mixture was dropwise added to BSA solution and stirred for pre-emulsification. Secondly, the emulsion was subjected to sonication at 300 W for 15 min with JY92-Ⅱ sonifier. Finally, the obtained magnetic microspheres were collected using a magnet. Then they were washed with ethanol and distilled water for removing the unreacted BSA.

2.2.2 Loading of GQDs with PTX

The PTX was loaded by adding 1.0 mL of PTX (1 mg/mL) to 30 mL of GQDs-NH_2 PBS buffer solution (0.5 mg/mL) under stirring for 24 h in the dark at room temperature. The obtained suspension was repeatedly dialyzed using dialysis bag with a molecular weight cutoff of 2 000 Da against PBS buffer for 24 h. The bath solution was changed with fresh PBS buffer every 4 h. And GQDs-NH_2 loading with PTX (PTX/GQDs-NH_2) was obtained.

2.2.3 Fluorescent modification of magnetic microspheres

To start fluorescent modification, firstly, 7.5 mg KAE/Fe_3O_4/BSA magnetic microspheres were added into the solution of 10 mg carbodiimide (EDC) and 8.6 mg N-hydroxysuccinimide (NHS) in 15 mL H_2O. Subsequently, the mixed solution was ultrasonically dispersed for 2 h, and 10 mL PTX/GQDs-NH_2 solution (0.3 mg/mL) was added. The resulting solution was stirred at room temperature for 12 h. Finally, the obtained MFDDs were collected by magnet, repeatedly washed by anhydrous ethanol and dried.

2.3 Characterization

The crystalline phase structure was determined by a Bruker D8 Advance X-ray diffractometer (XRD, D/max 18 kV) using Cu Kα radiation. Fourier-transform infrared (FT-IR) spectra of KBr powder pressed pellets

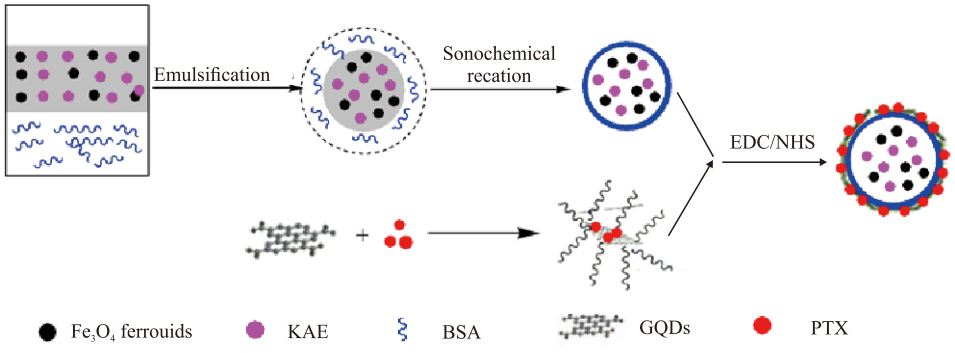

Fig.1 Schematic illustration of the formation processes of MFDDs

were recorded on a Bruker VECTOR 22 spectrometer. Transmission electron microscopy (TEM) and high-resolution transmission electron microscopy (HRTEM) images were recorded on a Tecnai 12 transmission electron microscope. And the magnetic property of sample was detected at room temperature by a vibrating sample magnetometer (VSM, Lake Shore 7410). X-ray fluorescence spectra (XRF, ARL-9800) were recorded by exciting the samples at 365 nm.

2.4 *In vitro* drug release from MFDDs

The release profiles of KAE or PTX from MFDDs were assessed in PBS at different pH values (7.4 and 5.0). Briefly, 10 mg MFDDs were suspended in 100 mL of the PBS release medium. The release experiment was started at 37 ℃ with continuous shaking at 100 rpm. At predetermined time, 3 mL of the incubated solution was withdrawn and replaced with equal volume of fresh PBS. The amount of KAE or PTX released was determined using a UV-visible spectrophotometer (UV1101M054), at wavelength of 370 or 230 nm. The drug loading efficiency and encapsulation efficiency were calculated using Eqs.(1) and (2), respectively:

$$\text{Drug loading efficiency}=\frac{m_d}{m_t}\times 100\% \quad (1)$$

$$\text{Encapsulation efficiency}=\frac{m_d}{m_0}\times 100\% \quad (2)$$

where m_d is the mass of KAE or PTX in the MFDDs, m_t is the total mass of MFDDs, and m_0 is the total mass of KAE or PTX. The calibration curves were plotted with a serial dilution of known concentrations of KAE or PTX in PBS, respectively.

2.5 *In vitro* cytotoxicity assasys

Hela cells were chosen to evaluate the *in vitro* cytotoxicity of MFDDs. Cells were cultured in Dulbecco's modified Eagle's medium (DMEM) supplemented with 10% (*v/v*) fetal bovine serum and 1% penicillin-streptomycin in a 5 % CO_2 incubator at 37 ℃. Before cytotoxicity tests, the samples were first sterilized in 75 % ethanol for 12 h, washed three times with sterile distilled water and PBS in sequence, and then dispersed in sterile PBS to produce dispersions.

100 μL of Hela cells were seeded in 96-well flat culture plate at a density of 1×10^5 cells per well and were subsequently incubated for 24 h to allow attachment. After that, samples with different concentrations were added to each group (six wells) for 24 h. As a blank, there were only the cells, and the cells were then incubated as before for an additional 24 h. Then 20 μL of a stock solution containing 15 mg 3-(4,5-dimethylthiazol-2-yl)-2,5-diphenyltetrazolium bromide (MTT) in 3 mL PBS was added and incubated for an additional 4 h. Finally, the medium was carefully removed, and 200 μL dimethyl sulfoxide (DMSO) was added to the cell, which was then properly shaken for 10 min. The absorbance was measured at a wavelength of 490 nm using Multiskan FC enzyme-labeled Instrument (Thermo Scientific, USA). The untreated cells were considered as control with 100 % viability[21]. The relative cell viability was determined using the following equation:

$$\text{Cell viability (\%)}=100\times\frac{A_{\text{test cells}}}{A_{\text{control cells}}} \quad (3)$$

Viable cells were also measured at day 3 by fluorescence microscopy (Olympus CKX41). The cells were incubated in 5 μg/mL fluorescein diacetate (FDA)/PBS solution for 10 min. During this process, FDA (no fluorescence) could penetrate through the cell membranes and was hydrolyzed into fluorescein by viable cells, which enabled the observation of the viable cells by excitation at 488 nm.

3 Results and discussion

3.1 Characterization of nanocomposites

MFDDs were synthesized by two procedures, illustrated in Fig.1. One is the synthesis of BSA functional magnetic microspheres by sonochemical method. In this procedure, Fe_3O_4 ferrofluids and KAE have clustered under the stability of BSA as a surfactant. At the same time, BSA molecules were adsorbed onto the surface of clusters to form inner shell under interface energy interaction. The other is the formation of PTX loaded GQDs (PTX/GQDs-NH_2) by π–π stacking. Finally, the covalent conjugation of PTX/GQDs-NH_2 onto the KAE/Fe_3O_4/BSA microspheres was achieved by forming peptide bond through coupling chemistry. So the MFDDs for co-delivery of KAE and PTX were obtained. In order to meet the demand of further biomedical application, the MFDDs were characterized as follows.

3.1.1 XRD analysis

Fig.2 shows the XRD patterns of (a) Fe_3O_4 ferrofluids and (b) KAE/Fe_3O_4/BSA microspheres. All the diffraction peaks marked in Fig.2(a) can be indexed to (220), (311), (400), (422), (511) and (440) planes of face-centered cubic Fe_3O_4 (JCPDS NO.89-2355). In Fig.2(b), the phase of magnetic component of KAE/Fe_3O_4/BSA microspheres was not altered because there

is no discernible shift in peak position between Fig.2(a) and Fig.2(b).

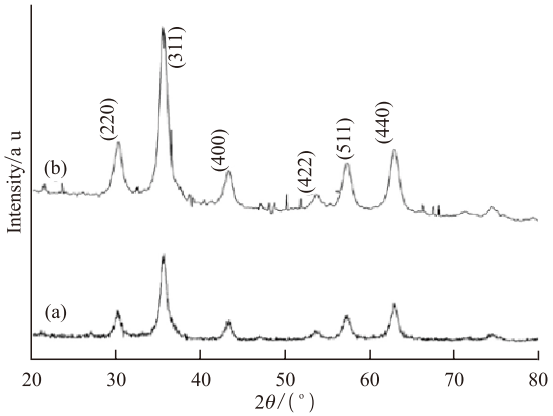

Fig.2 XRD patterns of (a) Fe_3O_4 ferrofluids and (b) KAE/Fe_3O_4/BSA microspheres

3.1.2 FT-IR analysis

In order to character the preparation process, the FT-IR spectra of (a) KAE/Fe_3O_4/BSA microspheres, (b) PTX/GQDs and (c) MFDDs are shown in Fig.3. In Fig.3(a), the characteristic absorption bands of -OH appeared at 3 421 cm^{-1}. The peaks at 1 604 cm^{-1} could be referred to the stretching vibration of C=O bond and the peaks at 1 400 cm^{-1} were attributed to the stretching vibration of C–N bonds. These results indicated that the functional groups (–CO–NH–) were located on the surface of magnetic microspheres[11]. So it was confirmed that the shell of magnetic microspheres was BSA. Moreover, the peaks at 1 175 and 1 046 cm^{-1} could be attributed to the presence of KAE, which confirmed that KAE was successfully loaded on magnetic microspheres.

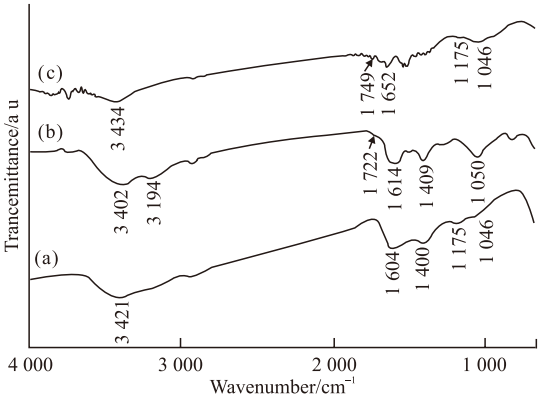

Fig.3 FT-IR spectra of: (a) KAE/Fe_3O_4/BSA microspheres, (b) PTX/GQDs and (c) MFDDs

In Fig.3(b), the appearance of double peaks centered around 3 402 and 3 194 cm^{-1} was corresponding to $–NH_2$[16]. According to the literature, the peaks at 1 614 and 1 722 cm^{-1} could be attributed to the presence of PTX[22], which showed that PTX was loaded on GQDs. In Fig.3(c), the bands at 3 434 cm^{-1} were attributed to the lapped peaks of N-H and O-H bonds. The peak at 1 749 cm^{-1} could be attributed to the presence of PTX, and the peaks at 1 175 and 1 046 cm^{-1} could be attributed to the presence of KAE. These results indicated that KAE and PTX were co-loaded on magnetic nanocomposites, and the MFDDs were obtained.

3.1.3 TEM analysis

Fig.4 shows the photographs of samples: (a) HR-TEM images of PTX/GQDs and (b) TEM images of MFDDs. In Fig.4(a), after loading with PTX, GQDs were still uniform and well dispersed. The particle size was in the range of 5-10 nm. And the ring-type diffraction pattern inserted in Fig.4(a) was indexed to polycrystalline GQDs. From Fig.4(b), the mean size of the MFDDs was calculated to be 110 nm. The uniformity in width of the polymer shell was related to the growth behavior of the polymer upon the rough surface of magnetic cores. Moreover, it was exhibited that the MFDDs had spherical structure, good dispersibility and sphericity which could be applied in subsequent experiments.

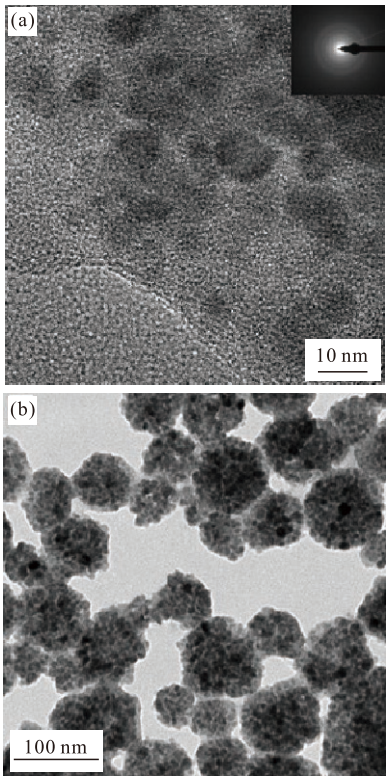

Fig.4 Photographs of samples: (a) HRTEM images of PTX/GQDs and (b) TEM images of MFDDs

3.1.4 VSM analysis

Furthermore, the room-temperature magnetic property of MFDDs was also examined by VSM. From

Fig.5, the product exhibited apparent superparamagnetism without any hysteresis[23]. The superparamagnetic behavior was also reflected in the low residual magnetization (M_r) and coercivity (H_c) values. Fig.5 shows that the saturation magnetization (M_s) of MFDDs was 24.36 emu/g, which was higher than that of magnetic microspheres (14.38 emu/g)[24]. When the external magnetic field was removed, MFDDs could be well dispersed by gentle shaking. These magnetic properties were critical for further biomedical application.

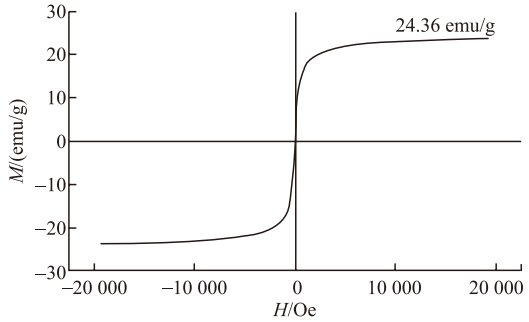

Fig.5 Magnetization curve of MFDDs

3.1.5 XRF analysis

To observe the fluorescence of MFDDs, a contrast experiment was designed. Fig.6 shows the fluorescence emission spectra of sample solutions at an excitation wavelength of 365 nm: (a) PTX/GQDs and (b) MFDDs. As observed in Fig.6(a), PTX/GQDs exhibited an intense emission peak at 446 nm. In Fig.6(b), it was found that the fluorescence intensity of the solution decreased with the decline of MFDDs concentration in the solution. As a result, it was concluded that we succeed in modifying GQDs/PTX on MFDDs[25].

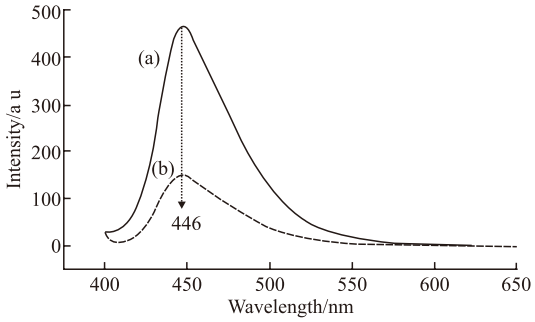

Fig.6 Fluorescence emission spectra of sample solutions at an excitation wavelength of 365 nm: (a) PTX/GQDs and (b) MFDDs

3.2 Drug release behavior

We have examined the *in vitro* release profiles of drugs from MFDDs at physiological pH (7.4) and at acidic pH (5.0). The relationship between absorbance (*Abs*) and drug concentration (*C*, μg/mL) could be respectively described by Eqs.(4) and (5):

$$Abs_{(KAE)} = 17.150 \cdot C_{(KAE)} + 0.0280,\ R^2 = 0.998 \quad (4)$$

$$Abs_{(PTX)} = 24.755 \cdot C_{(PTX)} + 0.158,\ R^2 = 0.996 \quad (5)$$

The data about drug loading and encapsulation efficiency were obtained by calculations based on the above equations. The drug loading and encapsulation efficiency of KAE were 2.85 μg/mg and 10.4 %, and the drug loading and encapsulation efficiency of PTX were 37.94 μg/mg and 58.8%, respectively.

The PTX and KAE release behaviors of MFDDs were assessed using a dialysis method at 37 ℃ in phosphate buffered saline (PBS) containing 0.1 % Tween 80 at different pH values. As shown in Fig.7(A), the release of PTX from MFDDs was greatly affected by the environmental acidity. After a 90 h incubation period, about 33.18% and 24.97 % of PTX were released at pH=5.5 and 7.4, respectively. The rapid PTX release at pH=5.5 might be attributed to the decreasing π–π stacking at low pH value.

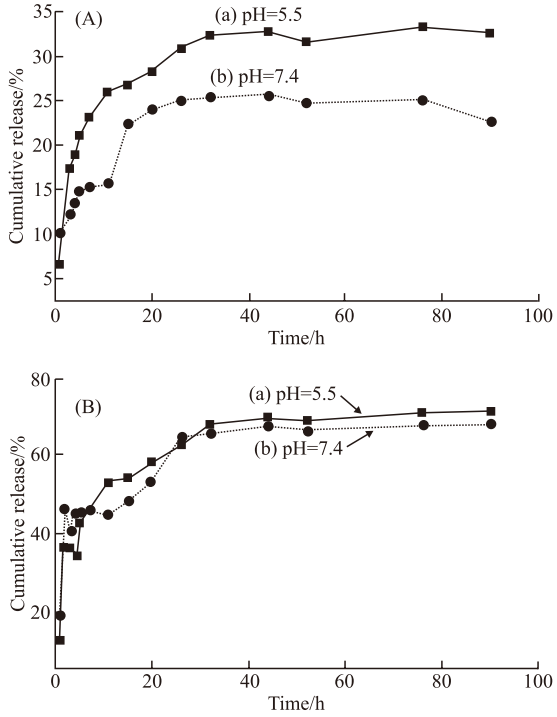

Fig.7 Release behaviors of: (A) PTX and (B) KAE from MFDDs at different pH values ((a) pH=5.5 and (b) pH=7.4) at 37 ℃

As shown in Fig.7(B), the release of KAE from MFDDs displayed a slow and sustained release pattern at different pH values. After a 90 h incubation period, about 70.41 % and 66.79 % of KAE were released at pH=5.5 and 7.4, respectively. Because BSA molecules in the shell were not significantly denatured[26], KAE was mainly released slowly through the BSA shell.

3.3 Cytotoxicity studies

The cytotoxicity of the drug-loaded carriers was tested by MTT assay in HeLa cells. Fig.8 shows the cytotoxicity of samples in Hela cells after 48 h of incubation: (a) KAE/Fe_3O_4/BSA microspheres (b) PTX/GQDs and (c) MFDDs. The data are shown in Fig.8(a), KAE/Fe_3O_4/BSA microspheres showed low cytotoxicity, and the IC_{50} in HeLa cells was about 10 μg/mL. As exhibited in Fig.8(b), a marked decrease in cell viability was watched when the Hela cells were incubated with PTX/GQDs. Even at 0.1 μg/mL, the cell viability rapidly decreased to 22.8%. Co-delivery of KAE and PTX by MFDDs further decreased the viability of HeLa cells. From Fig.8(c), when the concentration of MFDDs was 0.1 μg/mL, the cell viability rapidly decreased to 6.1%, which was much lower than that of KAE/Fe_3O_4/BSA microspheres (94.5%) and PTX/GQDs (22.8%). Previous literatures reported that the combination delivery of multi-drugs could improve the therapy efficacy as compared to the single therapeutic agent strategy[27]. Although the reason of this issue has not been entirely understood yet, the co-delivery strategy actually improved the anti-tumor efficacy *in vitro*.

Fluorescence microscopic images shown in Fig.9 confirmed the cell viability results, where the control group (Fig.9(a)) had the largest number of viable cells. In Fig.9(b), the number of viable cells decreased rapidly with the concentration of MFDDs (0.01 μg/mL), resulting in obvious morphological change of Hela cells. When the concentration of MFDDs increased to

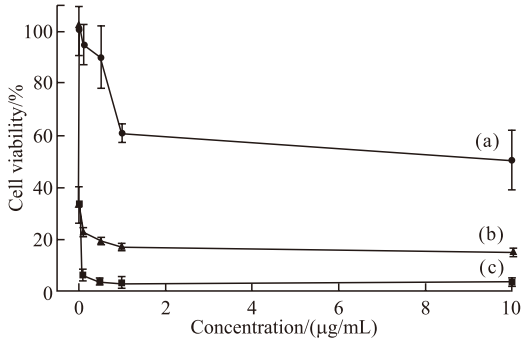

Fig.8 Cytotoxicity of the samples in Hela cells after 48 h of incubation: (a) KAE/Fe_3O_4/BSA microspheres, (b) PTX/GQDs and (c) MFDDs

0.1 and 10 μg/mL, only few cell clusters were found (Fig.9(c) and Fig.9(d)). In addition, with the same addition concentration of 0.1 μg/mL, there was no obvious morphological change of Hela cells observed in the presence of KAE/Fe_3O_4/BSA microspheres (Fig.9(e)). And at 0.1 μg/mL, the numbers of cells cultured on PTX/GQDs (Fig.9(f)) and MFDDs (Fig.9(c)) decreased significantly, especially on the surface of MFFDs. All these results confirmed that the MFDDs exhibited high anticaner activity for Hela cells than single drug carrier, which can be used as promising materials for targeted chemotherapy of cancer.

4 Conclusions

In summary, the magnetic fluorescent dual-drug nanocomposites loaded with KAE and PTX were successfully synthesized. The procedure was well-con-

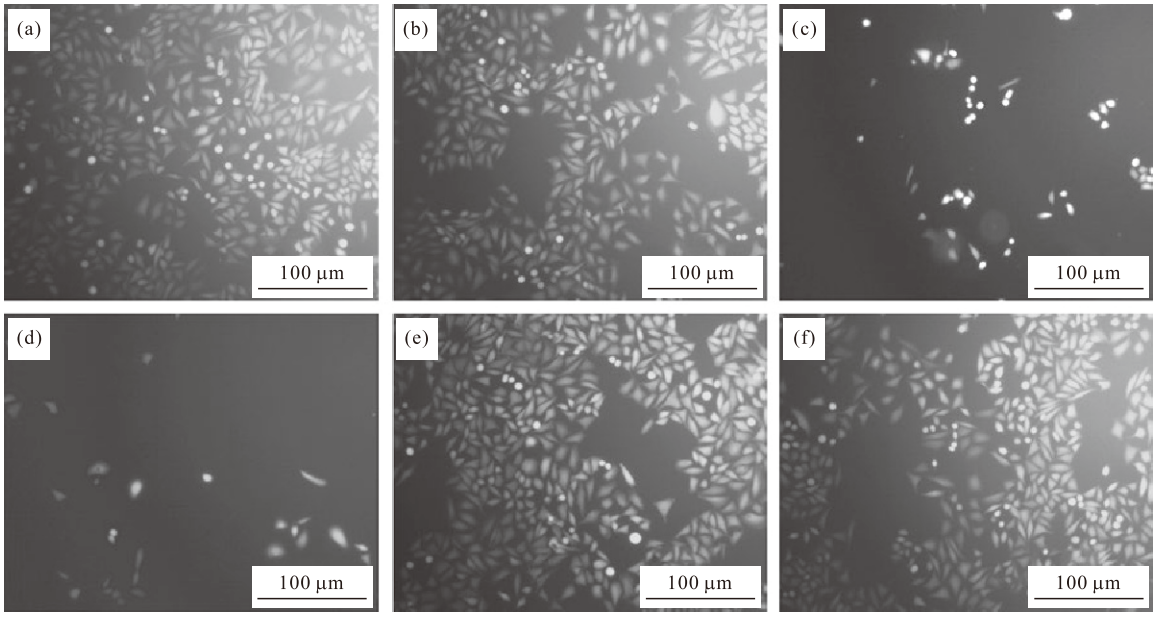

Fig.9 Hela cells observed by fluorescence microscopy after the cells were cultured on (a) the control (untreated) and (b-d) the MFDDs with different concentration of (b) 0.01 μg/mL, (c) 0.1 μg/mL, (d) 10 μg/mL. And with the same addition concentration of 0.1 μg/mL, cells on (c) MFFDs, (e) KAE/Fe_3O_4/BSA microspheres, (f) PTX/GQDs (Cell seeding density was 1×10^5 per well)

trolled and could be potentially applied to the preparation of multi-drug loading delivery systems with the purpose of overcoming multi-drug resistance. The as-obtained MFDDs revealed a certain sustained release effect, and could effectively inhibit the growth of Hela cells with low particle concentration (0.01 μg/mL). Consequently, such MFDDs were suggested to be efficient carrier for magnetically targeted combined chemotherapy of cancer. Besides, further works are now in progress in our laboratory.

References

[1] Duncan R. Polymer Conjugates as Anticancer Nanomedicines[J]. *Nat. Rev. Cancer*, 2006, 6: 688-701

[2] Duong H H P, Yung L Y L. Synergistic Co-delivery of Doxorubicin and Paclitaxel using Multi-functional Micelles for Cancer Treatment[J]. *Int. J. Pharm*., 2013, 454(1): 486-495

[3] Blackwell K L, Burstein H J, Storniolo A M, *et al.* Randomized Study of Lapatinib Alone or in Combination with Trastuzumab in Women with ErbB2-positive, Trastuzumab-refractory Metastatic Breast Cancer[J]. *J. Clin. Oncol*., 2010, 28(7): 1124-1130

[4] Salehi R, Rasouli S, Hamishehkar H. Smart Thermo/pH Responsive Magnetic Nanogels for the Simultaneous Delivery of Doxorubicin and Methotrexate[J]. *Int. J. Pharm.*, 2015, 487(1-2): 274-284

[5] Huang L, Song J C, Chen B Y. A Novel Targeting Drug Carrier to Deliver Chemical Bonded and Physical Entrapped Anti-tumor Drugs[J]. *Int. J. Pharm.*, 2014, 466(1-2): 52-57

[6] Pradhan L, Srivastava R, Bahadur D. pH- and Thermosensitive Thin Lipid Layer Coated Mesoporous Magnetic Nanoassemblies as a Dual Drug Delivery System towards Thermochemotherapy of Cancer[J]. *Acta Biomater*., 2014, 10(7): 2 976-2 987

[7] Ashwanikumar N, Kumar N A, Nair S A, *et al.* Dual Drug Delivery of 5-Fluorouracil (5-FU) and Methotrexate (MTX) through Random Copolymeric Nanomicelles of PLGA and Polyethylenimine Demonstrating Enhanced Cell Uptake and Cytotoxicity[J]. *Colloid. Surface B*, 2014, 122: 520-528

[8] Calabrò F, Lorusso V, Rosati G, *et al.* Gemcitabine and Paclitaxel Every 2 Weeks in Patients with Previously Untreated Urothelial Carcinoma[J]. *Cancer*, 2009, 115(12): 2 652-2 659

[9] Marfe G, Tafani M, Indelicato M, *et al.* Kaempferol Induces Apoptosis in Two Different Cell Lines via Akt Inactivation, Bax and SIRT3 Activation, and Mitochondrial Dysfunction[J]. *J. Cell. Biochem*., 2009, 106(4): 643-650

[10] Xu W, Liu J, Li C, *et al.* Kaempferol-7-O-*β*-d-glucoside (KG) Isolated from Smilax China L. Rhizome Induces G_2/M Phase Arrest and Apoptosis on HeLa Cells in a p53-independent Manner[J]. *Cancer Lett*., 2008, 264(2): 229-240

[11] Zhang X, Huang Y, Zhao W, *et al.* PEG-farnesyl Thiosalicylic Acid Telodendrimer Micelles as an Improved Formulation for Targeted Delivery of Paclitaxel[J]. *Mol. Pharm*., 2014, 11(8): 2 807-2 814

[12] Limtrakul P, Khantamat O, Pintha K. Inhibition of P-glycoprotein Function and Expression by Kaempferol and Quercetin[J]. *J. Chemother.*, 2005, 17(1): 86-95

[13] Chong Y, Ma Y, Shen H, *et al.* The *in Vitro* and *in Vivo* Toxicity of Graphene Quantum Dots[J]. *Biomaterials*, 2014, 35(19): 5 041-5 048

[14] Nahain A A, Lee J E, In I, *et al.* Target Delivery and Cell Imaging using Hyaluronic Acid-functionalized Graphene Quantum Dots[J]. *Mol. Pharmaceutics*, 2013, 10(10): 3 736-3 744

[15] Huang C L, Huang C C, Mai F D, *et al.* Application of Paramagnetic Graphene Quantum Dots as a Platform for Simultaneous Dual-modality Bioimaging and Tumor-targeted Drug Delivery[J]. *J. Mater. Chem. B*, 2014, 3: 651-664

[16] Jiang H H, Zhao L C, Gai L G, *et al.* Conjugation of Methotrexate onto Dedoped Fe_3O_4/PPy Nanospheres to Produce Magnetic Targeting Drug with Controlled Drug Release and Targeting Specificity for HeLa Cells[J]. *Synthetic Met*., 2015, 207: 18-25

[17] Ren Q, Chu H, Chen M, *et al.* Design and Fabrication of Superparamaganitic Hybrid Microspheres for Protein Immobilization[J]. *J. Wuhan Univ. Technol.-Mater. Sci. Ed.*, 2011, 26(6): 1 084-1 088

[18] Xu H X, Zhang Y, Niu X, *et al.* Preparation and *in Vitro* Release Properties of Mercaptopurine Drug-loaded Magnetic Microspheres[J]. *J. Wuhan Univ. Technol.-Mater. Sci. Ed*., 2013, 28(6): 1 231-1 235

[19] Zheng W, Gao F, Gu H. Magnetic Polymer Nanospheres with High and Uniform Magnetite Content[J]. *J. Magn. Magn. Mater.*, 2005, 288: 403-410

[20] Wang L, Wang Y, Xu T, *et al.* Gram-scale Synthesis of Single-crystalline Graphene Quantum Dots with Superior Optical Properties[J]. *Nat. Commun.*, 2014, 5: 5 357-5 357

[21] Navid M, Reza J M, Yahya H M, *et al.* Docetaxel-loaded Solid Lipid Nanoparticles: Preparation, Characterization, *in Vitro*, and *in Vivo* Evaluations[J]. *J. Pharm. Sci*., 2013, 102(6): 1 994-2 004

[22] Alipour S, Montaseri H, Tafaghodi M. Preparation and Characterization of Biodegradable Paclitaxel Loaded Alginate Microparticles for Pulmonary Delivery[J]. *Colloid. Surface B*, 2010, 81(2): 521-529

[23] Shamim N, Hong L, Hidajat K, *et al.* Thermosensitive Polymer (N-isopropylacrylamide) Coated Nanomagnetic Particles: Preparation and Characterization[J]. *Colloid. Surface B*, 2007, 55(1): 51-58

[24] Li F, Li X, Li B. Preparation of Magnetic Polylactic Acid Microspheres and Investigation of Its Releasing Property for Loading Curcumin[J]. *J. Magn. Magn. Mater.*, 2011, 323(22): 2 770-2 775

[25] Marcilene M A R, Andreza R S, Fernando L P, *et al.* Preparation, Characterization and *in Vitro* Cytotoxicity of BSA-based Nanospheres Containing Nanosized Magnetic Particles and/or Photosensitizer[J]. *J. Magn. Magn. Mater.*, 2009, 321: 1 600-1 603

[26] Avivi S, Gedanken A. The Preparation of Avidin Microspheres using the Snochemical Method and the Interaction of the Microspheres with Biotin[J]. *Ultrason. Sonochem*., 2005, 12(5): 405-409

[27] Youqing S, Erlei J, Bo Z, et al. Prodrugs Forming High Drug Loading Multifunctional Nanocapsules for Intracellular Cancer Drug Delivery-[J]. *J. Am. Chem. Soc.*, 2010, 132(12): 4 259-4 265